Broadband NMR relaxometry of electrolytes for energy storage

C. C. Fraenza and S.G. Greenbaum

Department of Physics & Astronomy

Hunter College of The City University of New York, 695 Park Avenue, New York, NY 10065

Abstract

An increasing use of the fast field cycling nuclear magnetic resonance relaxometry technique to investigate dynamics in electrolytes for energy storage has been evidenced during the last decade. Therefore, this review article describes some of the research carried out on electrolytes during the last ten years using this technique. These studies include various types of liquid electrolytes, such as ionic liquids and deep eutectic solvents, semi-solid-state electrolytes, in particular ionogels and polymer gels, and solid electrolytes such as glasses, glass ceramics and polymers. An extended description of the different models used to explain the relaxation rate profiles is presented throughout this article.

1. Introduction

Commercial lithium-ion (Li^+) batteries (LIBs) power an extraordinary range of devices from consumer electronics to the electrification of transportation and grid storage. However, efforts are ongoing to refine and improve their performance and thus develop the new generation of batteries that display substantial improvements in energy and power density, safety and reductions of environmental impacts and cost. This requires the right combination of electrodes and electrolyte, where the role of the latter is to act simultaneously as an ion conductor and electron insulator between the electrodes. Its electron-insulating property ensures that the charge transfer processes responsible for producing electricity takes place at the electrode-electrolyte interfaces, while its ion conducting property is directly related to the device's efficiency. The electrolyte can also affect the device's calendar and cycle life, electrochemical window of operation, capacity, safety, and other operating conditions.[1, 2] An ideal electrolyte should possess high ionic conductivity, thermal and electrochemical stability and should be non-volatile, non-flammable, non-toxic and biodegradable.[1, 2] There are various types of electrolytes which can be classified in categories as follows: liquid-containing electrolytes and dry solid electrolytes. Among the first ones include liquid electrolytes (aqueous and non-aqueous), ionogels and gel polymer electrolytes, whereas the second ones comprise inorganic solid electrolytes and solvent-free solid polymer electrolytes.

Considering the crucial role that electrolytes play in batteries, understanding the connection between structure and dynamics of them is thus at the heart of the effort to improve batteries' performance. Measurements of nuclear magnetic resonance (NMR) spin relaxations times[3-5] as a function of temperature and magnetic field strength (frequency) have become an important

investigative tool in the study of dynamics in materials.[6-16] The relaxation time that is most commonly measured in these studies is the spin-lattice relaxation time T_1 or relaxation rate $R_1=1/T_1$. T_1 is the characteristic time of the process by which the component of nuclear spin magnetization along the quantization field (M_o) builds up upon initially exposing a sample to a magnetic field B_o or returns to thermal equilibrium after being perturbed from equilibrium in B_o. This relaxation process is caused mainly by temporal fluctuations that the dipole-dipole (DD) interactions or, in the case of quadrupole nuclei, the interaction between quadrupole nuclei and the local electric field gradient (EFG) experience due to molecular motions.[3-5] If R_1 is measured as a function of frequency, it provides straightforward access to the frequency-dependent spectral density $J(\omega)$ according to[3, 17]:

$$R_1(\omega) = K[J(\omega) + 4J(2\omega)] \quad (1)$$

Here $\omega = 2\pi\nu$ is the angular frequency and $\nu = \gamma B_o/2\pi$ is the Larmor frequency, where γ is the gyromagnetic ratio of the nuclei; K is a constant that describes the strength of the dominating spin interaction, which can be dipolar ($K = A_{DD}$) or quadrupolar ($K = A_Q$); $J(\omega)$ is the Fourier transform of the time dependent correlation function $G(t)$ and provides information on the power spectrum of the fluctuations causing spin transitions. In the simplest case, $G(t)$ is given by a decaying exponential function and $J(\omega)$ exhibits a Lorentzian shape, as discussed by Bloembergen, Purcell, and Pound[17] and it is called the BPP model. However, this description is often inadequate requiring more complex models as described later in this manuscript.

Fast field cycling (FFC) relaxometry[18] is a non-destructive low-field NMR technique which is performed in the frequency range of a few kHz up to around 100 MHz, depending on the instrument. FFC-NMR is the only low-field NMR technique that measures R_1 at different values of the external magnetic field B_o (or Larmor frequency). Then, by using the Eq. (1) with an appropriate model for $J(\omega)$, it is possible to obtain information about the molecular dynamics of a material. It is worth mentioning that the relaxation time $T_{1\rho}$ can also be measured in the low-field (low frequency) range and it represents the time constant for the decay of magnetization along the radio frequency field, B_1, of an applied spin locking pulse in the rotating frame of reference.[3, 4] However, the range of frequencies at which the experiment can be performed is quite limited[19, 20] (from hundreds of Hz to a few tens of kHz).

In the FFC-NMR technique the strength of the magnetic field B_o is cycled by following three main steps as depicted in Fig. 1. Initially the magnetization is created in the sample via the application of a high polarization field B_P. Subsequently, in a few milliseconds the magnetic field is switched to a lower relaxation field B_R where the magnetization is allowed to relax during a period of time t_R. Finally, the magnetic field is switched to a higher field called detection field B_D where the remaining magnetization after the relaxation period t_R is acquired by applying a $\pi/2$ radio-frequency (RF) pulse. Then, this field cycle is repeated using different values of t_R and it is possible to calculate T_1 at the field B_R by fitting the magnetization $M(t_R)$ to an exponential decay. These measurements are repeated for several values of B_R, yielding $T_1(B_R)$ or equivalently $T_1(\omega)$.

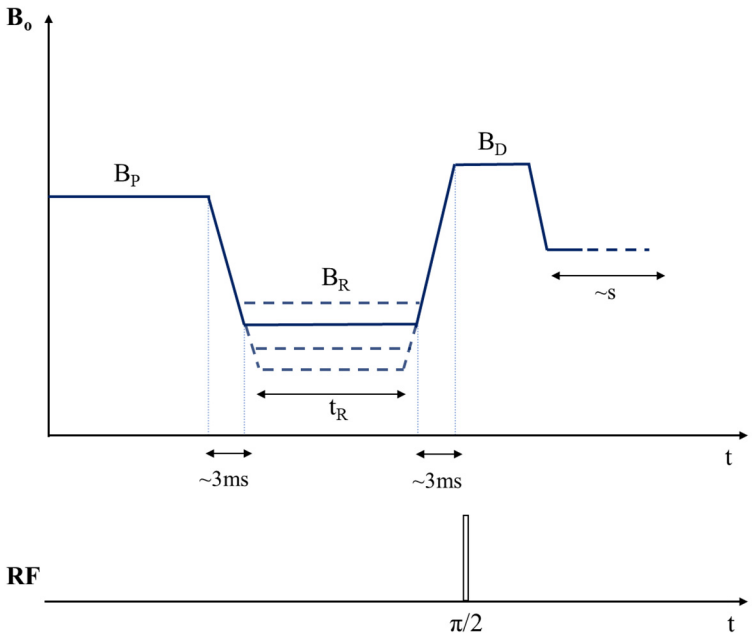

Figure 1. Diagram of a typical cycle of the main magnetic field B_o employed with fast field cycling NMR relaxometry. The remaining magnetization after the relaxation interval t_R is recorded in the form of a free induction decay (FID) after a $\pi/2$ RF pulse in the detection field B_D. The cycle is repeated after 4-5 times the spin–lattice relaxation time in the polarization field.

Throughout the last decade an increasing use of the FFC-NMR technique to investigate dynamics in electrolytes for energy storage has been evidenced.[15, 16, 21-33] Thus, this review article highlights some of this research carried out during the last ten years. Specifically covered are studies on liquid electrolytes, such as ionic liquids and deep eutectic solvents; on semi-solid-state electrolytes, such as ionogels and polymer gels, and solid electrolytes such as glasses, glass ceramics and polymers. In all cases, the models used to describe the spectral densities will be specified throughout this article.

2. Translational and rotational dynamics in liquid electrolytes

2.1. Ionic Liquids (ILs)

Ionic liquid-based electrolytes have gained increasing attention in the last decade because they seem to be promising candidates as an electrolyte for high performance batteries, when partnered with an appropriate lithium salt.[34-40] ILs are salts that melt commonly below 100ºC. They possess many useful properties, including low volatility, a broad liquid-state temperature window, low to zero flammability, wide electrochemical ranges (up to 6V), and fairly good ionic conductivities. The most used ILs consist of imidazolium-based cations[15, 16, 22, 23, 26-28, 31, 41-49] such as 1-butyl-3-methylimidazolium (BMIM, $[C_8H_{15}N_2]^+$) and 1-ethyl-3- methylimidazolium (EMIM, $[C_6H_{11}N_2]^+$).

On the other hand, the most commonly used anions include bis(trifluoromethylsulfonyl)imide[15, 23, 32, 46, 49] (TFSI, $[(CF_3SO_2)_2N]^-$), hexafluorophosphate[22, 47] ($[PF_6]^-$) and tetrafluoroborate[22] ($[BF_4]^-$).

FFC-NMR relaxometry technique has been widely used to study translational and rotational molecular motions of ions in ILs[15, 16, 22, 23, 26, 27, 31, 32, 46, 49-52]. In spite of the fact that this is a low-resolution technique, dynamics of cations and anions can be studied independently if they are composed of different NMR active nuclei.[16, 22, 27, 47, 49] For example, in the case of the IL [BMIM]PF_6, measuring the spin-lattice relaxation rate of ^1H and ^{19}F is equivalent to investigating molecular dynamics of $BMIM^+$ and PF_6^-, respectively.[22]

In general, temporal fluctuations of intramolecular and intermolecular DD interactions are the dominant relaxation mechanism in liquids composed of molecules carrying nuclear spins with I = ½ such as ^1H and ^{19}F and these fluctuations are caused by molecular motions such as rotations and translational diffusion.[3] Thus, in the case of ILs the spin-lattice relaxation rate dispersions can be described by considering these two molecular motions as a first approach. It is important to mention that oftentimes it is assumed that intermolecular relaxation is entirely controlled by translational diffusion. However, in ILs sometimes ions of opposite charge exhibit correlated motions and then the intermolecular relaxation is also governed by reorientations of transient charge-neutral ion couples, at low temperatures.[47] As temperature increases, the ion couples start breaking up and the dynamics displays an increasing contribution from free ions with intermolecular relaxation dominated by translational diffusion. This approach can be assumed when a similarity of the relaxation profiles for each ion type is observed across several temperatures and these profiles can be characterized by the same correlation times, even when the cation is much larger.[47]

Intramolecular and intermolecular dipolar interactions generally fluctuate in time at different time scales and therefore they are effective for spin-lattice relaxation in different regions of the frequency window of a FFC-NMR experiment. Specifically, intermolecular interaction fluctuations, which mostly depend on translational motion, dominate the spin-lattice relaxation in the low Larmor frequency regime while the effect of intramolecular interaction fluctuations shows up at high frequencies. Then, independently of the model used to describe the complete relaxation profile, it is possible to express the spin-lattice relaxation rate as a function of Larmor frequency v in the limit of low frequencies as $R_1(v) \cong B - A\sqrt{v}$, where A and B are constants. B represents the intramolecular contribution to relaxation which is not frequency dependent at low frequencies because it is mostly affected by fast molecular rotations and they are effective for relaxation at higher frequencies. A is given by[53-55]:

$$A = \left(\frac{\mu_0}{4\pi}\right)^2 n\,\gamma^4\hbar^2\left(\frac{8\sqrt{2}+2}{15}\right)\left(\frac{\pi}{D_{12}}\right)^{3/2} \quad (2)$$

Here μ_o is the permeability of free space, γ is the gyromagnetic ratio, n is the nuclear density and D_{12} is the relative diffusion coefficient defined as the sum of the self-diffusion coefficients of the involved molecular-pair ($D_{12} = D_1 + D_2$). If the two molecules are identical, D_{12} is equal to two

times the self-diffusion coefficient. Thus, if the values of R_1 are plotted against the square root of ν and fitted by Eq. (2) at lower frequencies, the diffusion coefficient can be calculated from the parameter A. This approach is an alternative to calculate the diffusion coefficients of the ions in ILs and it has been shown that these values are in agreement with the ones obtained with the standard pulsed field gradient (PFG-NMR) diffusion technique.[22, 31, 46]

The effect of translational diffusion on the intermolecular ^{1}H and ^{19}F spin-lattice relaxation in ILs has been successfully described[15, 16, 22, 23, 26, 27, 31, 32, 56, 57] by the force-free-hard-sphere (FFHS) model. FFHS model[53, 54] is a simple model which assumes that molecules behave as rigid spheres with their spins positioned in the center of them and they obey the Fick's diffusion equation. This model considers the excluded volume effect by defining a distance of closest approach d between two nuclei located in different molecules which is a way to neglect DD interactions for interspin distances that are shorter than d. The general expression of R_1 for three-dimensional translational diffusion given by the FFHS model is as follows[53]:

$$R_{1Diff} = \frac{108}{5}\left(\frac{\mu_0}{4\pi}\gamma^2 h\right)\frac{1}{d^3} n \int_0^\infty \frac{u^4}{81+9u^2-2u^4+u^6}\left[\frac{\tau_{Diff}}{u^4+(\omega\tau_{Diff})^2} + \frac{4\tau_{Diff}}{u^4+(2\omega\tau_{Diff})^2}\right] du \quad (3)$$

where u is a dimensionless integration variable, $\tau_{Diff} = \frac{d^2}{D_{12}}$ and D_{12} is the relative diffusion coefficient. It is possible to simplify Eq. (3) by assuming that diffusion is represented by finite jumps that have a mean square distance $r^2 \equiv 6D\tau$, where τ is the mean time between jumps and D is the self-diffusion coefficient. Thus, in the Brownian limit $r^2/6d^2 \rightarrow 0$, the homonuclear translational relaxation rate is given by[3, 58]:

$$R_{1Diff}^{ii}(\omega_i) = \frac{A_D^{ii}}{d_{ii}D_{ii}}\left[\tilde{J}\left(z(\omega_i)\right) + 4\tilde{J}\left(z(2\omega_i)\right)\right] \quad (4)$$

Here $\omega = 2\pi\nu$ and ν is the Larmor frequency; $A_D = \frac{8}{45}\pi\gamma^4\hbar^2\left(\frac{\mu_0}{4\pi}\right)^2 n$; $z(\omega) \equiv \sqrt{2\omega d^2/D_{12}}$, and $\tilde{J}(z) = \frac{1+\frac{5}{8}z+\frac{z^2}{8}}{1+z+\frac{z^2}{2}+\frac{z^3}{6}+\frac{z^5}{81}+\frac{z^6}{648}}$. On the other hand, if there is intermolecular DD interaction between two different types of nuclei, the heteronuclear translational relaxation rate takes the following expression[3, 58]:

$$R_{1Diff}^{ij}(\omega_i) = \frac{A_D^{ij}}{d_{ij}D_{ij}}\left[\tilde{J}\left(z(\omega_i-\omega_j)\right) + 3\tilde{J}\left(z(\omega_i)\right) + 6\tilde{J}\left(z(\omega_i+\omega_j)\right)\right] \quad (5)$$

Here $A_D^{ij} = \frac{1}{9}\gamma_i^2\gamma_j^2\hbar^2\left(\frac{\mu_0}{4\pi}\right)^2 n_j$, and the subscripts i and j refer to the two different nuclei. Translational ^{1}H and ^{19}F spin-lattice relaxation in IL-based electrolytes has been very well described by Eq. (4) and (5) in the following cases: [BMIM]TFSI with up to 1M LiTFSI at the temperature range of 303-333K[15] and [P_{4441}]TFSI (tributyl methyl phosphonium bis(trifluoromethanesulfonyl)imide)) and [N_{4441}]TFSI (tributyl methyl ammonium

bis(trifluoromethanesulfonyl)imide) with up to 0.6 molal concentration of LiTFSI at different temperatures in the range 298-338 K.[32]

On the other hand, the effect of rotational motion on intramolecular interactions can be described by a Lorentzian function (L) if it is assumed that rotations are isotropic with an average correlation time τ_R. Therefore, the rotational contribution to the spin-lattice relaxation rate is given by[3, 5, 17]:

$$R_{1rot}^{L}(\omega) = A_R \left[\frac{\tau_R}{1+(\omega)^2\tau_R{}^2} + \frac{4\tau_R}{1+(2\omega)^2\tau_R{}^2}\right] \quad (6)$$

Here $A_R = \frac{3}{10}\gamma^4\hbar^2\left(\frac{\mu_0}{4\pi}\right)^2\frac{1}{r^6}$ is the corresponding amplitude reflecting the strength of the relevant dipolar interactions and r is the effective distance between two nuclei located in the same molecule. This is the simplest model that can be used for rotational relaxation in liquids, however it has been used to successfully describe intramolecular relaxation in ILs and IL-based electrolytes.[15, 16, 23, 26, 32, 56, 57] There are improved models for rotational relaxation that have more complex mathematical expressions and are more realistic because they take into account the high viscosity of ILs and the anisotropic shape of ions and they consider a distribution of rotational correlation times. These models have been used to depict intramolecular relaxation in ILs.[22, 27, 28] One of them is the Cole-Davidson (CD) model[22, 27, 31, 59] which describes the rotational motion as thermally activated jumps over a distribution of potential barriers and the rotational contribution to relaxation has the following expression in this case:

$$R_{1rot}^{CD}(\omega) = A_R \left[\frac{\sin(\beta \arctan(\omega\tau_{CD}))}{\omega(1+(\omega\tau_{CD})^2)^{\beta/2}} + \frac{2\sin(\beta \arctan(2\omega\tau_{CD}))}{\omega(1+(2\omega\tau_{CD})^2)^{\beta/2}}\right] \quad (7)$$

where τ_{CD} is the average correlation time, $0 < \beta \leq 1$ is a phenomenological stretching parameter indicating the spread of correlation times (Eq. (7) takes a Lorentzian form with only one correlation time if $\beta = 1$) and $\tau_R = \beta\tau_{CD}$.

Another model is the Woessner's model[60] (W) which takes into account anisotropic reorientations that elongated ions experience by defining two different correlation times for reorientations around the short (τ_S) and long (τ_L) molecular axes and the rotational relaxation rate is given by the following equation:

$$R_{1rot}^{W}(\omega) = A_R[J^W(\omega) + 4J^W(2\omega)] \quad (8)$$

Here $J^W(\omega) = \frac{2}{15}\left[A_0\frac{2\tau_1}{1+(\omega\tau_1)^2} + A_1\frac{2\tau_2}{1+(\omega\tau_2)^2} + A_2\frac{2\tau_3}{1+(\omega\tau_3)^2}\right]$; $\tau_1 = \tau_S$, $\tau_2 = (1/\tau_S + 1/\tau_L)^{-1}$ and $\tau_3 = (1/\tau_S + 4/\tau_L)^{-1}$; the parameters $A_0 = (1-3cos^2\alpha)^2/4$, $A_1 = 3sin^2\alpha/4$ and $A_2 = 3sin^4\alpha/4$ are the geometric factors depending on the angle α between the $\boldsymbol{r}$ vector (r is the intramolecular distance between two nuclei) and the long axis of the molecule. This model has been used to describe rotational relaxation of $BMIM^+$ in the ILs BMIMCl[28] and [BMIM][BF_4].[24]

As it was mentioned before, in general translational and rotational motions are dominant in different time scales and can be considered statistically independent. Therefore, the total spin-lattice relaxation rate of ILs will be given by:

$$R_{1IL}^{I=½}(\omega) = R_{1intra}(\omega) + R_{1inter}(\omega) = R_{1rot}(\omega) + R_{1Diff}^{ii}(\omega) + R_{1Diff}^{ij}(\omega) \quad (9)$$

where the superscripts *ii* and *ij* stand for homonuclear and heteronuclear translational relaxation, respectively. Many works have addressed the measured relaxation rate dispersions of nuclei with $I = ½$, such as ^{1}H and ^{19}F, in ILs by using Eq. (9).[15, 16, 22, 23, 26-28, 31, 32, 56, 57]

In the case of IL-based electrolytes, which are composed of an IL partnered with a lithium salt, many studies have used broadband NMR relaxometry to mostly investigate dipolar relaxation of ions in the IL but a few of them have analyzed the quadrupolar relaxation of ^{7}Li in the salt.[15] Considering that ^{7}Li has a quadrupolar nucleus because of its spin $I = 3/2 \geq 1$, ^{7}Li spin-lattice relaxation is mainly caused by temporal fluctuations of the interaction between the nuclear electric quadrupole Q and the EFG tensor originated from the surrounding intra and intermolecular charge distributions. There is a study that has investigated the molecular dynamics of all ions in the electrolyte made of [BMIM] TFSI with up to 1M LiTFSI and considered that the local translational motion of Li^{+} within the coordination sphere surrounded by anions is the main mechanism causing temporal fluctuations of the EFG tensor.[15] Thus, the spin-lattice relaxation rate of lithium can be expressed by a Lorentzian function if isotropic diffusional motion given by jumps with an average correlation time τ_{jump} is assumed[15]:

$$R_{1IL}^{Li}(\omega) = A_Q \left[\frac{\tau_{jump}}{1+(\omega)^2 {\tau_{jump}}^2} + \frac{4\tau_{jump}}{1+(2\omega)^2 {\tau_{jump}}^2} \right] \quad (10)$$

Here $A_Q = \frac{3\pi^2}{10} \frac{(2I+3)}{I^2(2I-1)} \left(1 + \frac{\eta^3}{3}\right)^2 C_Q^2$, where η is the asymmetry parameter of the EFG and $\eta=0$ if it is assumed that the EFG tensor is axially symmetric; $\tau_{jump} \equiv \langle r \rangle^2 / 6D_j$, $\langle r \rangle^2$ is the average one-jump distance and D_j is the diffusion coefficient; C_Q is the quadrupolar coupling constant.

As an alternative, molecular dynamics simulations (MDS) can be helpful to identify proper relaxation models given that they do not make model assumptions to calculate dynamical parameters such as diffusion coefficients and rotational correlation times. Therefore, there are some works that have made a comparison between broadband relaxometry experiments and MDS in the case of ILs.[56, 57] It has been demonstrated that the dispersion curves of ^{1}H spin-lattice relaxation rate can be simulated with good accuracy for $EMIM^{+}$ in the IL [EMIM][$N(CN)_2$] (1-ethyl-3-methylimidazolium dicyanamide) at the temperature range of 260-340K.[56] Additionally, it was shown that the values and temperature trends of diffusion constants and correlation times obtained from the experiment and simulation were in good agreement for the cation in the IL [TEA]TFSI (triethylammonium bis(trifluoromethylsulfonyl)imide).[57] This result demonstrated that the assumptions made by using the FFHS and BPP models to describe translational and rotational relaxation respectively are applicable. However, it was also shown that in the case of

ions that exhibit strongly anisotropic reorientational dynamics such as $TFSI^-$, assuming isotropic reorientations described by the BPP model with a single correlation time could not be appropriate and at least two different correlation times are necessary.

2.2. Deep Eutectic Solvents (DESs)

Deep eutectic solvents[61, 62], which sometimes are called "quasi-ionic liquids" or "ionic liquid analogues" due to their similar properties, have shown to be promising candidates as electrolytes as well.[63-71] These solvents are defined as a mixture of two or more species, typically a hydrogen bond donor (HBD) species and a hydrogen bond acceptor (HBA) species, which may be solid or liquid and that combine to yield a melting temperature that is significantly below the melting points of the parent compounds. Unlike typical ILs, DESs can be inexpensive, readily synthesized, and can often be prepared from biodegradable, and nontoxic constituents.[72, 73]

Although NMR spectroscopy has been used to study DESs[67, 74-79], the use of FFC-NMR is in its infancy with very few examples to highlight.[33] Among the most used DESs are the ones composed of choline chloride (ChCl) as HBA[74-79] and glycerol[74-76, 78], ethylene glycol (EG)[75, 76, 78, 79], phenol[79] or urea[75, 76, 78] as HBD. There are a few NMR relaxometry studies of dynamics of pure EG[80] and glycerol[81-83], however there are only two works that have used FFC-NMR to investigate DESs.

Specifically, one of them has studied the effect of different water concentrations (0, 0.1, 1, 10, and 28.5 wt %) on the dynamics of the DES ethaline (a 1:2 mol % mixture of ChCl and EG) by using different experimental techniques such as femtosecond time-resolved absorption spectroscopy (fs-TA), broadband dielectric spectroscopy (BDS), NMR diffusometry and broadband relaxometry, and MDS.[33] Although ethaline is known to be very hygroscopic and water absorption can alter its properties, it has been demonstrated that adding small amounts of water between 1 to 10wt% can improve the charge transport properties of the solvent instead of being a concern. Contrary, if water content is smaller than 1wt%, the dynamics of the solvent slow down which indicates than the attempt to dry ethaline can be counterproductive if the goal is to accomplish a high-performing electrolyte solution. ^{1}H NMR diffusometry and broadband relaxometry results have showed that translational and rotational motions of choline and EG in ethaline accelerate with the presence of water, and the higher the water content, the faster these motions become. This is a direct consequence of the decreasing viscosity when water is added. In this work, the ^{1}H spin-lattice relaxation of choline and EG has been successfully described by using the models given by Eq. (4), (6) and (9). Additionally, these models have been used in a second paper to describe the ^{1}H spin-lattice relaxation of choline and glycerol in the DES glyceline (a 1:2 mol % mixture of ChCl and glycerol) very well. This work, which is from the same research group, combines multiple NMR techniques such as FFC relaxometry, PFG diffusion, nuclear overhauser effect spectroscopy (NOESY), ^{13}C NMR relaxation and pressure dependent NMR experiments to sample a range of frequencies and modes of motion of glycerol and choline in glyceline and has recently been submitted for publication.

3. Translational and rotational dynamics in confined liquid electrolytes

Broadband relaxometry has also been used to investigate molecular motions in confined IL-based electrolytes such as ionogels and gel polymer electrolytes[15, 16, 24, 26, 28, 32, 84-86] as well as confined aqueous electrolyte solutions.[87] In the case of confined IL-based electrolytes, some of these studies have focused only on the dynamics of the cation[24, 28, 84, 85, 87] and others have studied both cation and anion dynamics.[15, 16, 26, 32, 86] Depending on the type of confining matrix and how it interacts with ions, a slight slowing-down[28] or enhancement[24, 84, 87] of the ion dynamics and ionic conductivity can be observed under confinement.

It has been shown that, independently of the type of IL, the spin-lattice relaxation rate profiles of bulk IL-based electrolytes present no frequency dependence in the low frequency window (in general below 1 MHz).[15, 16, 24, 26, 28, 32, 84-87] But, when this IL electrolyte is confined, a well-pronounced dispersion is seen in this frequency range because of the interactions between the ions and the confining material. An example of this is shown in Fig. 2 which compares the dispersions of the ^{1}H spin-lattice relaxation rate of two ILs ([P4441]TFSI and [N4441]TFSI) without and with LiTFSI (0.6 m) to the relaxation profiles of the gel polymer electrolyte made of these ILs electrolytes and polymethyl methacrylate (PMMA) polymer at 10 wt. %.[32]

3.1. Ionogels (IGs)

An IG consists of an IL confined in a mesoporous inorganic matrix which macroscopically behaves as a solid, but at the nanoscale a liquid-like state is maintained.[88] Thus, IGs overcome the safety issues due to possible leakage of ILs and exhibit the high mechanical strength of the solid matrix. Among the most commonly used confining materials in relaxometry studies are the SiO_2 matrix[15, 16, 26, 85] and Vycor porous glass.[86]

The molecular dynamics of IGs can be quite complex and depending on the composition of the IL and confining matrix and on the relative size of the ions and the cavities of the matrix, the dynamic properties of the confined IL can be very different. Thus, two approaches have been considered to describe the spin-lattice relaxation dispersions of IGs. Specifically, they have been called the two and one ion population approaches.

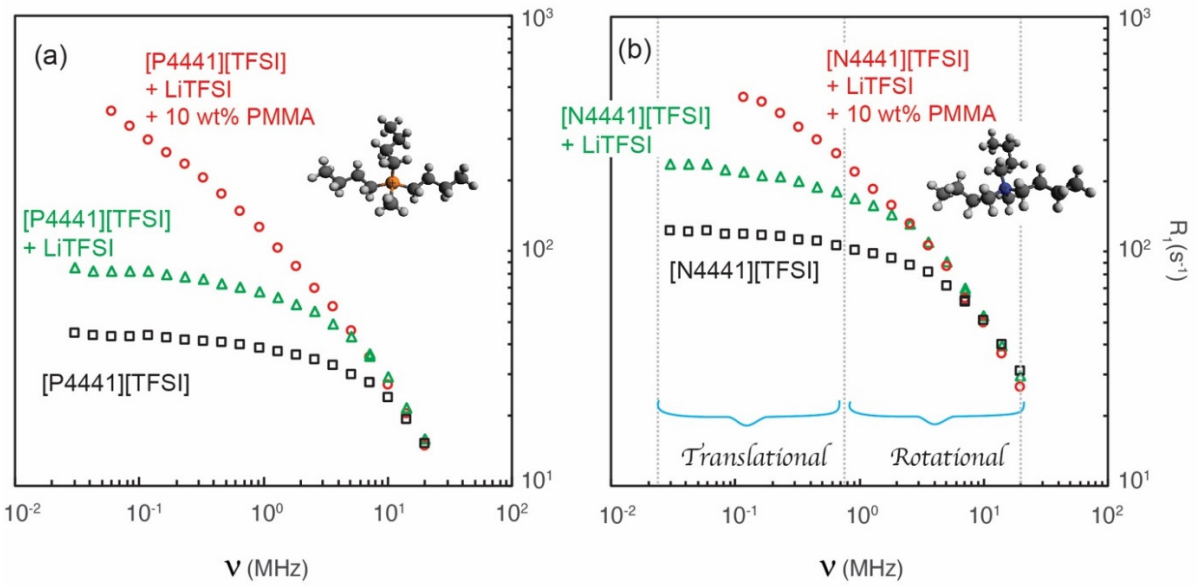

Figure 2. ^{1}H spin-lattice relaxation rate profiles of the ILs **(a)** [P4441]TFSI and **(b)** [N4441]TFSI without and with LiTFSI (0.6m) and the polymer gel electrolytes made of polymethyl methacrylate (PMMA) polymer at 10 wt. % and these IL electrolytes. A well-pronounced dispersion at low frequencies is observed when the IL electrolytes are confined. **Reproduced/Adapted from Ref. 32 with permission from Elsevier, Copyright 2021.**

Two-population approach

The two ion population approach assumes that, as a consequence of the confinement, there are two different fractions of ions: the bulk-like fraction and the surface fraction.[26, 85, 87] The first one, which is dominant, comprises ions that move almost freely near the cavity center as if there was no confinement. On the other hand, the surface fraction consists of ions that interact with the cavity walls and their dynamics are affected by the topology of the matrix surface. The bulk-like fraction can be also identified as ions at least a few ionic radii distant from the matrix surfaces and the surface fraction as those ions close to the matrix surfaces.[15] It is worth mentioning that the distinction of these two fractions of ions is only possible under the assumption that the size of the cavities of the matrix is big enough. Thus, if it is assumed that the residence lifetime of the ions on the surface is longer than the translational correlation time in bulk, the total relaxation rate can be written as follows:

$$R_{1IG}^{2\ populations}(\omega) = R_1^{core}(\omega) + R_1^{surf}(\omega) \tag{11}$$

The existence of these two ion populations can be supported by direct measurement of the diffusion coefficients D^{core} and D^{surf} with their corresponding weight factors by using PFG-NMR and in this way the two fractions of the liquid can be expressed explicitly by multiplying each term of Eq. (11) by these weight factors.[15] The spin-lattice relaxation rate of ions that belong to the bulk-like fraction (R_1^{core}) can be described by the Eq. (9) or (10), depending on the value of the quantum

number I of the nuclei.[15, 26, 85, 87] Whereas, the relaxation of ions that are part of the surface fraction (R_1^{surf}) can be explained in two different manners. One of them assumes that R_1^{surf} is also given by the models of Eq. (9) or (10) and the total relaxation rate has the following expression[26, 85]:

$$R_{1IG}^{2\ populations} = R_1^{core}(\omega) + R_1^{surf}(\omega) = R_{1Diff}^{core}(\omega) + R_{1Rot}^{core}(\omega) + R_{1Diff}^{surf}(\omega) + R_{1Rot}^{surf}(\omega) \quad (12)$$

where there are four different dynamic parameters involved, namely, D^{core}, D^{surf}, τ_R^{core} and τ_R^{surf}. On the other hand, the other manner to describe R_1^{surf} takes into account the restricted translational motion that it is experienced by the ions that interact with the confining material and assumes that the main relaxation mechanism is the molecular reorientations mediated by translational displacements (RMTD).[15, 87] These reorientations occur on a much slower time scale than bulk rotational or translational diffusion and they take place when the solvent and the surface are polar. Then, the total relaxation rate is given by:

$$R_{1IG}^{2\ populations} = R_1^{core}(\omega) + R_1^{surf}(\omega) = R_{1Diff}^{core}(\omega) + R_{1Rot}^{core}(\omega) + R_{1RMTD}^{surf}(\omega) \quad (13)$$

where:

$$R_{1RMTD}^{surf}(\omega) = A_{RMTD}[J^{RMTD}(\omega) + 4J^{RMTD}(2\omega)] \quad (14)$$

A_{RMTD} is a constant that depends on, among others, the geometrical features of the confining material and on the fraction of molecules at the surface, and J^{RMTD} can be expressed as follows[89]:

$$J^{RMTD}(\omega) = \frac{1}{(2\pi)^2}\int_0^\infty S(k)\frac{2\tau_k}{1+(\omega\tau_k)^2}dk \quad (15)$$

where k and τ_k are the wave number and time constant of diffusion modes, respectively, and $S(k)$ is the orientational structure factor which depicts the geometrical information of the surface in terms of these modes. The expressions of $S(k)$ and $\tau_k(k)$ depend on the assumptions that are made. If it is assumed that the diffusion of ions in the surface fraction is two-dimensional, represented by a Gaussian probability density[89] and there is an equipartition of the wave numbers describing different diffusion modes ($S(k)$ is a constant)[15, 87, 89], $R_{1RMTD}^{surf}(\omega)$ is given by:

$$R_{1RMTD}^{surf}(\omega) = A_{RMTD}\left[\omega^{-0.5}\left(f\left(\frac{\omega_{max}}{\omega}\right) - f\left(\frac{\omega_{min}}{\omega}\right)\right) + 4(2\omega)^{-0.5}\left(f\left(\frac{\omega_{max}}{2\omega}\right) - f\left(\frac{\omega_{min}}{2\omega}\right)\right)\right] \quad (16)$$

where $f(\omega) = \arctan((2\omega)^{0.5} + 1) + \arctan((2\omega)^{0.5} - 1) - \text{arctanh}\left(\frac{(2\omega)^{0.5}}{\omega+1}\right)$; $\omega_{min} = \frac{4D_{surf}}{l_{max}^2}$ and $\omega_{max} = \frac{4D_{surf}}{l_{min}^2}$ are, respectively, the minimum and maximum frequencies of diffusion modes; D_{surf} denotes the surface diffusion coefficient, and l_{min} and l_{max} represent the smallest and largest displacement distance along the surface, respectively. The two-population approach using Eq. (13) and (16) has been applied to successfully describe relaxation profiles in the following cases: i) ^{1}H

and ^{19}F spin-lattice relaxation profiles in the IG made of the IL electrolyte composed of [BMIM]TFSI with the lithium salt LiTFSI (up to 1M) confined in a silica matrix[15]; ii) ^{1}H relaxation in the gel electrolyte composed of an aqueous solution of the tetramethylammonium bromide salt (TMABr) confined into a matrix made of a low molecular weight gelator.[87]

Alternatively, it is often assumed that $S(k)$ follows a power law and $R_{1RMTD}^{surf}(\omega)$ takes the following expression[89]:

$$R_{1RMTD}^{surf}(\omega) = \widetilde{A_{RMTD}}\omega^{-p}, \quad 0 < p < 1 \tag{17}$$

$\widetilde{A_{RMTD}}$ is an amplitude that can be expressed in terms of the diffusion constant by the equation: $\widetilde{A_{RMTD}} = C \times (D_{surf})^{p-1}$, where C is a constant that depends on the type of spin interaction, on the exponent p and on the type of probability density.[89] The two-population approach using Eq. (10) and (17) has been applied to describe the spin-lattice relaxation rate profiles of the quadrupolar nucleus ^{7}Li in the IG made of the IL electrolyte [BMIM]TFSI with LiTFSI confined into a SiO_2 matrix.[15]

One-population approach

The one-population approach considers that it is not possible to distinguish two different populations of ions due to the small dimensions of cavities and all ions interact with the confining walls all the time. In this case, the total relaxation rate of IG is given by:

$$R_{1IG}^{1\,population}(\omega) = R_{1RMTD}^{surf}(\omega) \tag{18}$$

Here $R_{1RMTD}^{surf}(\omega)$ can be described by Eq. (16) or (17) depending on the assumptions that are made. This approach, using Eq. (17), has been applied to describe the ^{1}H and ^{19}F spin-lattice relaxation profiles of the IL [BMIM]TFSI confined into a porous glass.[86]

Conversely, the ^{1}H and ^{19}F spin-lattice relaxation profiles of the IG made of the IL [EMIM]FSI confined into a mesoporous MCM41 silica matrix have been explained by assuming that the main relaxation mechanisms are two-dimensional (2D) translational diffusion and molecular rotations.[16] The 2D diffusion was considered as taking place when the ions are near the confining walls where they describe loops with interruptions if they are attached to the surface for some time. Whereas, the rotational motion of the confined ions was considered as anisotropic and thus described by two correlation times. Then, the total relaxation rate in this case is given by[16]:

$$R_{1IG}^{1\,population} = R_1^{2D\,Diff}(\omega) + R_1^{Rot,s}(\omega) + R_1^{Rot,f}(\omega) + R_1^{FM} \tag{19}$$

Here $R_1^{2D\,Diff}(\omega) = A_{trans}\tau_{trans}\left[\ln\left(1+\frac{1}{(\omega\tau_{trans})^2}\right) + 4\ln(1+\frac{1}{(2\omega\tau_{trans})^2})\right]$; $R_1^{Rot,s}(\omega)$ and $R_1^{Rot,f}(\omega)$ follows a Lorentzian form (Eq. (6)) and the superscripts *s* and *f* stand for slow and fast rotations, respectively. R_1^{FM} is a frequency independent term which is associated with all dynamical

processes that are too fast, such as internal dynamics of the ions, to show any dispersion on the frequency window of the experiment.

3.2. Gel polymer electrolytes (GPEs)

GPEs[90, 91] consist of a gelled polymer matrix swollen by a liquid electrolyte and due to their optimal interfacing with electrodes and liquid-like transport behavior, they have found application in commercial LIBs. Broadband NMR relaxometry has been used to study GPEs made of confined IL-based electrolytes[24, 28, 32] and, in the same way as IGs, the dynamic properties of ILs in confinement strongly depend on the relative size of the ions and the cavities, and on the specific IL and polymer composition. Therefore, the same two different approaches used for IGs (i.e., the two and one ion population approaches), have been considered as well to describe the spin-lattice relaxation rate dispersions of GPEs.

The two-population approach has been used to study $BMIM^+$ dynamics in two different GPEs which are described below. One of them was made of bisphenol A ethoxylate dimethacrylate (bisAEA4) and [BMIM]BF_4 at the mass ratio of 20:80.[24] The ^1H spin-lattice relaxation rate profile of the cation was measured and successfully explained by the model of Eq. (13), in the range of temperatures 248-343K. The "bulk-like" fraction was described in terms of translational diffusion using the Torrey model[92] and anisotropic molecular rotations using Woessner's model (Eq. (8)). Whereas, the fraction of cations interacting with the polymer was described by the RMTD model given by Eq. (16). The diffusion coefficients obtained from the analysis of the relaxation profiles showed that their largest values were for the ions interacting with the polymer. This was consistent with the additional ionic conductivity results obtained via electrochemical impedance spectroscopy, which revealed that the value of ionic conductivity for GPE was twice higher than that of bulk IL. The authors speculated that the interaction of the IL with the polymer decreased the size of ion aggregates and their tendency to be formed in the IL/polymer interface, allowing ions to create new ionic-conducting pathway, which might explain the observed conductivity enhancement under confinement of the IL. On the other hand, the second GPE was made of BMIMCl and cellulose (Cell) at 10wt%.[28] The ^1H spin-lattice relaxation rate profiles of $BMIM^+$ was measured in the range of temperatures 298-368K and described by exactly the same model used by the paper presented above in this paragraph.[24] It was shown that the gelation only results in a small decrease of the ion conductivity by comparing conductivity measurements performed for bulk IL and IL confined in the Cell/BMIMCl GPE. It is interesting to notice how crucial the composition of the GPE is to determine the conductivity properties, which is clearly evidenced in the two works described above.

The one-population approach has been used to study the cation and anion dynamics in two different GPEs made of polymethyl methacrylate (PMMA) polymer at 10 wt. % and the ILs [P_{4441}]TFSI or [N_{4441}]TFSI, both with up to 0.6 molal concentration of LiTFSI.[32] The ^1H and ^{19}F spin-lattice relaxation rate profiles were measured at different temperatures and modeled by the RMTD model (Eq. (16)). For cation relaxation a Lorentzian term (Eq. (6)) was added to the model to take into account molecular reorientations of cations that happen when they do not interact with

the polymer. It was shown that confinement caused a mild slow-down in the dynamics of ions and cations experienced a less restricted motion than anions because of the more probable interaction between anions and the polymer. As an example, these relaxation profiles and their corresponding fittings for the polymer gel electrolyte made of PMMA polymer at 10 wt. % and [N4441]TFSI +0.6m LiTFSI at 298K are presented in Fig. 3.

As shown in the two previous paragraphs, there are some studies that have investigated relaxation of dipolar nuclei, such as ^{1}H and ^{19}F, in GPEs but studies about relaxation of the quadrupolar nucleus ^{7}Li in GPEs are scarce. There is a work that has analyzed the influence of the polymer on the local dynamics of lithium ions in two ternary GPEs by using temperature dependent ^{7}Li R_1 measurements at a few frequencies.[93] The two GPEs were composed of 1-butyl-1-methylpyrrolidinium bis(trifluoromethanesulfonyl) imide (P_{14}TFSI), LiTFSI, and either polyethylene oxide (PEO) or poly(diallyldimethylammonium) TFSI (PDADMA-TFSI). The CD (Eq. (7)) and BPP (Eq. (6)) models were used to describe the ^{7}Li relaxation rates but, if a temperature dependent quadrupole coupling constant is considered, the CD model explained the data better. For both polymers the correlation times increased with polymer concentration because of the restricted movement caused by the polymer network. However, the activation energy of local motions slightly decreased for increasing PDADMA-TFSI concentration, which indicates that the reduction of local Li^+ motion was less effective in the $PDADMA^+$ samples. It was concluded that it is possible to compensate the reduced Li^+ motion under confinement by using a cationic polymer, such as PDADMA-TFSI, because it can induce breakup of lithium-anion clusters and in this way make Li^+ free.

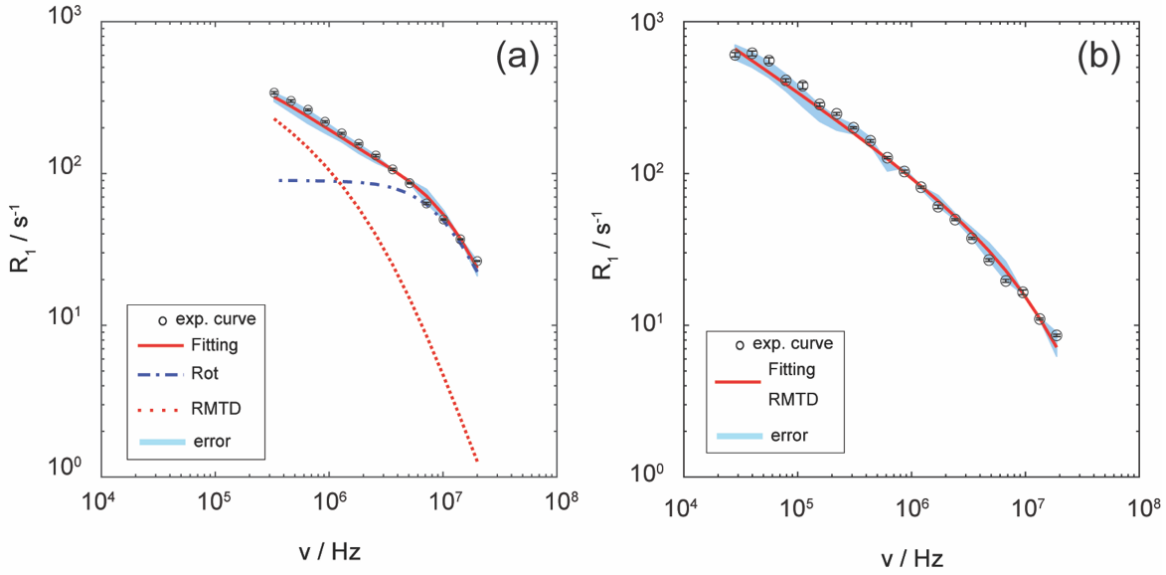

Figure 3. (a) ^{1}H and **(b)** ^{19}F spin-lattice relaxation rate profiles of the polymer gel electrolyte made of PMMA polymer at 10 wt. % and [N4441]TFSI +0.6m LiTFSI, measured at 298K. RMTD are the main relaxation mechanism for both nuclei, however, a Lorentzian term is added in the case of ^{1}H relaxation to consider molecular reorientations that take place when cations do not interact with the polymer. **Reproduced/Adapted from Ref. 32 with permission from Elsevier, Copyright 2021.**

4. Dynamics in solid electrolytes

The study of solid electrolytes using broadband NMR relaxometry is quite limited because of the following reasons, which are connected to electronic limitations. First, solids have in general short values of the spin-spin relaxation time T_2, which causes a very fast decay of the NMR signal and makes the signal measurement unfeasible. Second, the values of T_1 at low magnetic fields generally are shorter or in the same range of values than the switching time (2-3 ms) which makes T_1 measurement unreliable. However, a few works using FFC-NMR to investigate solid electrolytes such as glasses[21, 25], glass ceramics[29], and polymer electrolytes[30] have been reported, as described below.

^{7}Li FFC-NMR has been used to study lithium ion dynamics in the ternary $0.5Li_2S+0.5[(1–x)GeS_2+xGeO_2]$ glass system with x = 0 and 0.1, at different temperatures in the range 200-450K.[25] The ^{7}Li spin-lattice relaxation rate profiles were described by using two different models, namely, the multi-exponential (ME) autocorrelation function model and the power-law waiting time (PLWT) model. The ME model considers that the relaxation rate can be written as a superposition of Lorentzian functions with a distribution of the correlation times, $C(\tau_c)$, as follows:

$$R_{1glass_ME}^{Li}(\omega) = A_Q\left[\int_0^\infty C(\tau_c)\frac{\tau_c}{(1+\omega^2\tau_c^2)}d\tau_c + \int_0^\infty C(\tau_c)\frac{4\tau_c}{(1+(2\omega)^2\tau_c^2)}d\tau_c\right] \quad (20)$$

It was assumed that ion hops were thermally activated with correlation times that follow an Arrhenius relation and the activation energy has a temperature-independent distribution $g(E_A)$. Then, $C(\tau_c)$ is given by:

$$C(\tau_c) = \tau_o e^{\frac{g(E_A)}{k_B T}} \quad (21)$$

Here $g(E_A)$ is a Gaussian distribution, $g(E_A) = \frac{1}{\sigma\sqrt{2\pi}}e^{-\frac{(E_A-<E_A>)^2}{2\sigma^2}}$. This model described lithium relaxation very well for temperatures higher than 300K, which indicated a change in the ^{7}Li relaxation mechanism upon cooling. On the other hand, the PLWT considers that lithium ions move in the glass network according to a random walk in a random potential energy landscape[94, 95] and it leads to a Cole-Cole (CC) spectral density.[96] Then, the relaxation rate has the following expression:

$$R_{1glass_CC}^{Li}(\omega) = A_Q\left[\frac{4\omega^{\alpha-1}\tau_{CC}^{\alpha}\sin(\alpha\pi/2)}{4+4(\omega\tau_{CC})^{\alpha}\cos\left(\frac{\alpha\pi}{2}\right)+(\omega\tau_{CC})^{2\alpha}} + \frac{16\omega^{\alpha-1}\tau_{CC}^{\alpha}\sin(\alpha\pi/2)}{4+4(2\omega\tau_{CC})^{\alpha}\cos\left(\frac{\alpha\pi}{2}\right)+(2\omega\tau_{CC})^{2\alpha}}\right] \quad (22)$$

In this model there is a single time τ_{cc} and the parameter α measures the non-exponentiality of the dynamical process. ^{7}Li relaxation data was also well described by this model and then it was not possible to determine which model was better based on the available data.

Li^+ dynamics in the $0.7Li_2S–0.3P_2S_5$ glass (LiPS-GL) electrolyte has been studied by using a combination of ^{7}Li field-cycling relaxometry and stimulated-echo experiments, covering thereby

a time window extending over 10 orders of magnitude (10^{-9}-10^{1} s) without any gaps.[21] Both techniques revealed a pronounced non-exponentiality of the Li^+ hopping motion. Thus, the relaxation rate profiles at high temperatures were well described by the CD model (Eq. (7)). Subsequently, the glass-ceramic obtained from LiPS-GL after heat treatment at 553K for 1h (LiPS-GC) has been investigated.[29] ^{7}Li spin-lattice relaxation rate as a function of frequency and temperature was measured to characterize short-range ion jumps and static field gradient NMR was used to study long-range ion diffusion, in LiPS-GC. The ^{7}Li relaxation profiles were described by the ME model (Eq. (20)) because the correlation functions were strongly non-exponential. It was showed that ceramization substantially enhanced the Li^+ mobility on all length scales.

On the other hand, the polymer electrolyte made of unentangled poly(propylene glycol) (PPG) and lithium perchlorate ($LiClO_4$) or LiTFSI has been investigated.[30] The polymer and lithium ion dynamics were studied by using ^{1}H and ^{7}Li FFC relaxometry, respectively, at salts concentrations of 15:1 and 6:1 (ratio of polymer oxygens to lithium ions) and in the wide range of temperatures of 290-380K. It was assumed that the main relaxation mechanisms for ^{1}H relaxation in the polymer were segmental motion at short times ($R_{1CD}(\omega)$) and Rouse dynamics at longer times ($R_{1Rouse}(\omega)$). Thus, the total ^{1}H relaxation rate was described by a superposition of these two mechanisms as follows:

$$R_1^{Polymer}(\omega) = R_{1CD}(\omega) + R_{1Rouse}(\omega) \tag{23}$$

Here the segmental motion follows a CD form (Eq. (7)) and the contribution associated with Rouse dynamics is given by[97]:

$$R_{1Rouse}(\omega) = A_{Rouse}\tau_O \left[\sum_{p,q=1}^{N-1} \frac{p^2+q^2}{(p^2+q^2)^2+(\omega\tau_o N^2)^2} + 4\sum_{p,q=1}^{N-1} \frac{p^2+q^2}{(p^2+q^2)^2+(2\omega\tau_o N^2)^2}\right] \tag{24}$$

where A_{Rouse} is a constant that depends on the proton gyromagnetic ratio and on the mean interproton distance; N denotes the number of Rouse beads and τ_o is a time constant which is proportional to the friction coefficient of the Rouse model. The addition of salts caused an increase of correlation times and dynamical heterogeneity in the case of segmental motion. In fact, ^{1}H relaxation was described by a superposition of two CD functions in the case of 15:1 salt concentration because of the observed bimodal dynamics originated from the coexistence of two different regions, namely, salt-rich and salt-depleted regions. On the other hand, the ^{7}Li relaxation profiles were also described by using the model given by Eq. (23) because of the strong coupling of polymer and Li^+ dynamics that was observed. However, Li^+ dynamics was not bimodal which suggested that the majority of lithium ions were in the salt-rich regions and the very minor fraction in the salt-depleted regions could not be observed.

5. Conclusion

In this review the potentiality of broadband NMR relaxometry to study dynamics of electrolytes for energy storage has been shown and details of the various models used to interpret the relaxometry profiles have been described. Additionally, it has been evidenced that this technique can efficiently describe the connection between structural and dynamical aspects of different types of electrolytes. In some cases, a simple model, such as the BPP model, is able to explain the relaxation rate profile but in other cases more complex models, such as CD, ME, RMTD or Rouse models, are required. Relaxometry studies of ILs can probe the translational and rotational dynamics of cations and anions independently, in the cases that these ions are composed of different NMR active nuclei. Moreover, it has been demonstrated that modest amounts of water addition (1-10wt%) to the DES ethaline could lead to performance improvements by increasing mobility of constituents. On the other hand, relaxation profiles of specific types of confined IL electrolytes have revealed the existence of two different ion populations, namely "bulk-like" and "wall-interacting" fractions. Finally, relaxometry results have evidenced the nonexponentiality of Li^+ jump motion in different types of glasses, where models such as CD, ME and CC were used to describe the ^7Li relaxation profiles. Furthermore, it has been shown that ceramization substantially enhances the Li^+ mobility in glass-ceramic electrolytes. In summary, all these studies prove the breadth of application and the invaluable nature of broadband NMR relaxometry to characterize dynamics of electrolytes for energy storage.

Acknowledgement

This work was supported as part of the Breakthrough Electrolytes for Energy Storage (BEES), an Energy Frontier Research Center funded by the U.S. Department of Energy, Office of Science, Basic Energy Sciences under Award #: DE-SC0019409.

Data Availability

Data sharing is not applicable to this article as no new data were created or analyzed in this study.

References

1. Xu, K., Nonaqueous liquid electrolytes for lithium-based rechargeable batteries. *Chemical reviews* **2004,** *104* (10), 4303-4418.
2. Marcinek, M.; Syzdek, J.; Marczewski, M.; Piszcz, M.; Niedzicki, L.; Kalita, M.; Plewa-Marczewska, A.; Bitner, A.; Wieczorek, P.; Trzeciak, T., Electrolytes for Li-ion transport–Review. *Solid State Ionics* **2015,** *276*, 107-126.
3. Abragam, A., *The principles of nuclear magnetism*. Oxford university press: 1961.
4. Slichter, C. P., *Principles of Magnetic Resonance*. Springer Science & Business Media: 1996; Vol. 1.
5. Levitt, M. H., Spin dynamics: Basics of Nuclear Magnetic Resonance John Wiley & Sons. *New York-London-Sydney* **2008**.

6. Yasaka, Y.; Kimura, Y., Polarity and nonpolarity of ionic liquids viewed from the rotational dynamics of carbon monoxide. *The Journal of Physical Chemistry B* **2015,** *119* (50), 15493-15501.
7. Gouverneur, M.; Jeremias, S.; Schönhoff, M., 7Li nuclear magnetic resonance studies of dynamics in a ternary gel polymer electrolyte based on polymeric ionic liquids. *Electrochimica Acta* **2015,** *175*, 35-41.
8. Pope, C. R.; Romanenko, K.; MacFarlane, D. R.; Forsyth, M.; O'Dell, L. A., Sodium ion dynamics in a sulfonate based ionomer system studied by 23Na solid-state nuclear magnetic resonance and impedance spectroscopy. *Electrochimica Acta* **2015,** *175*, 62-67.
9. Rumble, C. A.; Kaintz, A.; Yadav, S. K.; Conway, B.; Araque, J. C.; Baker, G. A.; Margulis, C.; Maroncelli, M., Rotational dynamics in ionic liquids from NMR relaxation experiments and simulations: Benzene and 1-ethyl-3-methylimidazolium. *The Journal of Physical Chemistry B* **2016,** *120* (35), 9450-9467.
10. Richardson, P.; Voice, A.; Ward, I., NMR self diffusion and relaxation time measurements for poly (vinylidene fluoride)(PVDF) based polymer gel electrolytes containing LiBF4 and propylene carbonate. *Polymer* **2016,** *97*, 69-79.
11. Strate, A.; Neumann, J.; Overbeck, V.; Bonsa, A.-M.; Michalik, D.; Paschek, D.; Ludwig, R., Rotational and translational dynamics and their relation to hydrogen bond lifetimes in an ionic liquid by means of NMR relaxation time experiments and molecular dynamics simulation. *The Journal of chemical physics* **2018,** *148* (19), 193843.
12. Peng, J.; Gobet, M.; Devany, M.; Xu, K.; von Wald Cresce, A.; Borodin, O.; Greenbaum, S., Multinuclear magnetic resonance investigation of cation-anion and anion-solvent interactions in carbonate electrolytes. *Journal of Power Sources* **2018,** *399*, 215-222.
13. Chen, Y.; Jaegers, N. R.; Wang, H.; Han, K. S.; Hu, J. Z.; Mueller, K. T.; Murugesan, V., Role of Solvent Rearrangement on Mg2+ Solvation Structures in Dimethoxyethane Solutions using Multimodal NMR Analysis. *The Journal of Physical Chemistry Letters* **2020,** *11* (15), 6443-6449.
14. Zinkevich, T.; Fiedler, A.; Guin, M.; Tietz, F.; Guillon, O.; Ehrenberg, H.; Indris, S., Na+ ion mobility in Na3+ xSc2 (SiO4) x (PO4) 3− x (0.1< x< 0.8) observed by 23Na NMR spectroscopy. *Solid state ionics* **2020,** *348*, 115277.
15. Jayakody, N. K.; Fraenza, C. C.; Greenbaum, S. G.; Ashby, D.; Dunn, B. S., NMR relaxometry and diffusometry analysis of dynamics in ionic liquids and ionogels for use in lithium-ion batteries. *The Journal of Physical Chemistry B* **2020,** *124* (31), 6843-6856.
16. Kruk, D.; Wojciechowski, M.; Florek-Wojciechowska, M.; Singh, R. K., Dynamics of Ionic Liquids in Confinement by Means of NMR Relaxometry—EMIM-FSI in a Silica Matrix as an Example. *Materials* **2020,** *13* (19), 4351.
17. Bloembergen, N.; Purcell, E. M.; Pound, R. V., Relaxation effects in nuclear magnetic resonance absorption. *Physical review* **1948,** *73* (7), 679.
18. Kimmich, R.; Anoardo, E., Field-cycling NMR relaxometry. *Progress in Nuclear Magnetic Resonance Spectroscopy* **2004,** *44* (3), 257-320.
19. Kettunen, M.; Kauppinen, R.; Gröhn, O., Dispersion of cerebral on-resonanceT 1 in the rotating frame (T 1ρ) in global ischaemia. *Applied Magnetic Resonance* **2005,** *29* (1), 89-106.
20. Koskinen, S. K.; Niemi, P. T.; Kajander, S. A.; Komu, M. E., T1ρ dispersion profile of rat tissues in vitro at very low locking fields. *Magnetic resonance imaging* **2006,** *24* (3), 295-299.
21. Graf, M.; Kresse, B.; Privalov, A. F.; Vogel, M., Combining 7Li NMR field-cycling relaxometry and stimulated-echo experiments: A powerful approach to lithium ion dynamics in solid-state electrolytes. *Solid state nuclear magnetic resonance* **2013,** *51*, 25-30.
22. Kruk, D.; Meier, R.; Rachocki, A.; Korpała, A.; Singh, R.; Rössler, E., Determining diffusion coefficients of ionic liquids by means of field cycling nuclear magnetic resonance relaxometry. *The Journal of Chemical Physics* **2014,** *140* (24), 244509.

23. Seyedlar, A. O.; Stapf, S.; Mattea, C., Dynamics of the ionic liquid 1-butyl-3-methylimidazolium bis (trifluoromethylsulphonyl) imide studied by nuclear magnetic resonance dispersion and diffusion. *Physical Chemistry Chemical Physics* **2015,** *17* (3), 1653-1659.
24. Rachocki, A.; Andrzejewska, E.; Dembna, A.; Tritt-Goc, J., Translational dynamics of ionic liquid imidazolium cations at solid/liquid interface in gel polymer electrolyte. *European Polymer Journal* **2015,** *71*, 210-220.
25. Gabriel, J.; Petrov, O. V.; Kim, Y.; Martin, S. W.; Vogel, M., Lithium ion dynamics in Li2S+ GeS2+ GeO2 glasses studied using 7Li NMR field-cycling relaxometry and line-shape analysis. *Solid state nuclear magnetic resonance* **2015,** *70*, 53-62.
26. Kruk, D.; Wojciechowski, M.; Brym, S.; Singh, R. K., Dynamics of ionic liquids in bulk and in confinement by means of 1 H NMR relaxometry–BMIM-OcSO 4 in an SiO 2 matrix as an example. *Physical Chemistry Chemical Physics* **2016,** *18* (33), 23184-23194.
27. Wencka, M.; Apih, T.; Korošec, R. C.; Jenczyk, J.; Jarek, M.; Szutkowski, K.; Jurga, S.; Dolinšek, J., Molecular dynamics of 1-ethyl-3-methylimidazolium triflate ionic liquid studied by 1 H and 19 F nuclear magnetic resonances. *Physical Chemistry Chemical Physics* **2017,** *19* (23), 15368-15376.
28. Kaszyńska, J.; Rachocki, A.; Bielejewski, M.; Tritt-Goc, J., Influence of cellulose gel matrix on BMIMCl ionic liquid dynamics and conductivity. *Cellulose* **2017,** *24* (4), 1641-1655.
29. Haaks, M.; Martin, S. W.; Vogel, M., Relation of short-range and long-range lithium ion dynamics in glass-ceramics: Insights from Li 7 NMR field-cycling and field-gradient studies. *Physical Review B* **2017,** *96* (10), 104301.
30. Becher, M.; Becker, S.; Hecht, L.; Vogel, M., From local to diffusive dynamics in polymer electrolytes: NMR studies on coupling of polymer and ion dynamics across length and time scales. *Macromolecules* **2019,** *52* (23), 9128-9139.
31. Overbeck, V.; Appelhagen, A.; Rößler, R.; Niemann, T.; Ludwig, R., Rotational correlation times, diffusion coefficients and quadrupolar peaks of the protic ionic liquid ethylammonium nitrate by means of 1H fast field cycling NMR relaxometry. *Journal of Molecular Liquids* **2021,** *322*, 114983.
32. Garaga, M. N.; Jayakody, N.; Fraenza, C. C.; Itin, B.; Greenbaum, S., Molecular-level insights into structure and dynamics in ionic liquids and polymer gel electrolytes. *Journal of Molecular Liquids* **2021,** *329*, 115454.
33. Alfurayj, I.; Fraenza, C. C.; Zhang, Y.; Pandian, R.; Spittle, S.; Hansen, B.; Dean, W.; Gurkan, B.; Savinell, R.; Greenbaum, S., Solvation Dynamics of Wet Ethaline: Water is the Magic Component. *The Journal of Physical Chemistry B* **2021**.
34. Navarra, M. A., Ionic liquids as safe electrolyte components for Li-metal and Li-ion batteries. *MRS bulletin* **2013,** *38* (7), 548-553.
35. Zhao, Y.; Bostrom, T., Application of ionic liquids in solar cells and batteries: a review. *Current Organic Chemistry* **2015,** *19* (6), 556-566.
36. Eftekhari, A.; Liu, Y.; Chen, P., Different roles of ionic liquids in lithium batteries. *Journal of Power Sources* **2016,** *334*, 221-239.
37. Watanabe, M.; Thomas, M. L.; Zhang, S.; Ueno, K.; Yasuda, T.; Dokko, K., Application of ionic liquids to energy storage and conversion materials and devices. *Chemical reviews* **2017,** *117* (10), 7190-7239.
38. Rüther, T.; Bhatt, A. I.; Best, A. S.; Harris, K. R.; Hollenkamp, A. F., Electrolytes for lithium (sodium) batteries based on ionic liquids: highlighting the key role played by the anion. *Batteries & Supercaps* **2020,** *3* (9), 793-827.
39. Liu, K.; Wang, Z.; Shi, L.; Jungsuttiwong, S.; Yuan, S., Ionic liquids for high performance lithium metal batteries. *Journal of Energy Chemistry* **2020**.
40. Stettner, T.; Balducci, A., Protic ionic liquids in energy storage devices: Past, present and future perspective. *Energy Storage Materials* **2021**.

41. Suarez, S. N.; Rúa, A.; Cuffari, D.; Pilar, K.; Hatcher, J. L.; Ramati, S.; Wishart, J. F., Do TFSA anions slither? Pressure exposes the role of TFSA conformational exchange in self-diffusion. *The Journal of Physical Chemistry B* **2015,** *119* (46), 14756-14765.
42. Yoshimura, Y.; Shigemi, M.; Takaku, M.; Yamamura, M.; Takekiyo, T.; Abe, H.; Hamaya, N.; Wakabayashi, D.; Nishida, K.; Funamori, N., Stability of the liquid state of imidazolium-based ionic liquids under high pressure at room temperature. *The Journal of Physical Chemistry B* **2015,** *119* (25), 8146-8153.
43. Harris, K. R.; Kanakubo, M., Self-diffusion, velocity cross-correlation, distinct diffusion and resistance coefficients of the ionic liquid [BMIM][Tf 2 N] at high pressure. *Physical Chemistry Chemical Physics* **2015,** *17* (37), 23977-23993.
44. Nazet, A.; Sokolov, S.; Sonnleitner, T.; Makino, T.; Kanakubo, M.; Buchner, R., Densities, viscosities, and conductivities of the imidazolium ionic liquids [Emim][Ac],[Emim][FAP],[Bmim][BETI],[Bmim][FSI],[Hmim][TFSI], and [Omim][TFSI]. *Journal of Chemical & Engineering Data* **2015,** *60* (8), 2400-2411.
45. Brooks, N. J.; Castiglione, F.; Doherty, C. M.; Dolan, A.; Hill, A. J.; Hunt, P. A.; Matthews, R. P.; Mauri, M.; Mele, A.; Simonutti, R., Linking the structures, free volumes, and properties of ionic liquid mixtures. *Chemical science* **2017,** *8* (9), 6359-6374.
46. Pilar, K.; Rua, A.; Suarez, S. N.; Mallia, C.; Lai, S.; Jayakody, J.; Hatcher, J. L.; Wishart, J. F.; Greenbaum, S., Investigation of dynamics in BMIM TFSA ionic liquid through variable temperature and pressure NMR relaxometry and diffusometry. *Journal of the Electrochemical Society* **2017,** *164* (8), H5189.
47. Driver, G. W.; Huang, Y.; Laaksonen, A.; Sparrman, T.; Wang, Y.-L.; Westlund, P.-O., Correlated/non-correlated ion dynamics of charge-neutral ion couples: the origin of ionicity in ionic liquids. *Physical Chemistry Chemical Physics* **2017,** *19* (7), 4975-4988.
48. Ordikhani Seyedlar, A.; Stapf, S.; Mattea, C., Cation dynamics in supercooled and solid alkyl methylimidazolium bromide ionic liquids. *The Journal of Physical Chemistry B* **2017,** *121* (21), 5363-5373.
49. Becher, M.; Steinrücken, E.; Vogel, M., On the relation between reorientation and diffusion in glass-forming ionic liquids with micro-heterogeneous structures. *The Journal of chemical physics* **2019,** *151* (19), 194503.
50. Daniel, C. I.; Vaca Chávez, F. n.; Feio, G.; Portugal, C. A.; Crespo, J. G.; Sebastião, P. J., 1H NMR relaxometry, viscometry, and PFG NMR studies of magnetic and nonmagnetic ionic liquids. *The Journal of Physical Chemistry B* **2013,** *117* (39), 11877-11884.
51. Beira, M.; Daniel, C. I.; Almeida, P. L.; Corvo, M. C.; Rosatella, A. A.; Afonso, C. A.; Sebastião, P. J., 1H NMR Relaxometry and Diffusometry Study of Magnetic and Nonmagnetic Ionic Liquid-Based Solutions: Cosolvent and Temperature Effects. *The Journal of Physical Chemistry B* **2017,** *121* (51), 11472-11484.
52. Kruk, D.; Masiewicz, E.; Lotarska, S.; Markiewicz, R.; Jurga, S., Correlated Dynamics in Ionic Liquids by Means of NMR Relaxometry: Butyltriethylammonium bis (Trifluoromethanesulfonyl) imide as an Example. *International journal of molecular sciences* **2021,** *22* (17), 9117.
53. Hwang, L. P.; Freed, J. H., Dynamic effects of pair correlation functions on spin relaxation by translational diffusion in liquids. *The Journal of Chemical Physics* **1975,** *63* (9), 4017-4025.
54. Ayant, Y.; Belorizky, E.; Aluzon, J.; Gallice, J., Calcul des densités spectrales résultant d'un mouvement aléatoire de translation en relaxation par interaction dipolaire magnétique dans les liquides. *Journal de Physique* **1975,** *36* (10), 991-1004.
55. Sholl, C., Nuclear spin relaxation by translational diffusion in liquids and solids: high-and low-frequency limits. *Journal of Physics C: Solid State Physics* **1981,** *14* (4), 447.
56. Honegger, P.; Overbeck, V.; Strate, A.; Appelhagen, A.; Sappl, M.; Heid, E.; Schröder, C.; Ludwig, R.; Steinhauser, O., Understanding the nature of nuclear magnetic resonance relaxation by

means of fast-field-cycling relaxometry and molecular dynamics simulations—the validity of relaxation models. *The journal of physical chemistry letters* **2020,** *11* (6), 2165-2170.
57. Overbeck, V.; Golub, B.; Schroeder, H.; Appelhagen, A.; Paschek, D.; Neymeyr, K.; Ludwig, R., Probing relaxation models by means of Fast Field-Cycling relaxometry, NMR spectroscopy and molecular dynamics simulations: Detailed insight into the translational and rotational dynamics of a protic ionic liquid. *Journal of Molecular Liquids* **2020,** *319*, 114207.
58. Freed, J. H., Dynamic effects of pair correlation functions on spin relaxation by translational diffusion in liquids. II. Finite jumps and independent T 1 processes. *The Journal of Chemical Physics* **1978,** *68* (9), 4034-4037.
59. Davidson, D. W.; Cole, R. H., Dielectric relaxation in glycerol, propylene glycol, and n-propanol. *The Journal of Chemical Physics* **1951,** *19* (12), 1484-1490.
60. Woessner, D., Spin relaxation processes in a two-proton system undergoing anisotropic reorientation. *The Journal of Chemical Physics* **1962,** *36* (1), 1-4.
61. Smith, E. L.; Abbott, A. P.; Ryder, K. S., Deep eutectic solvents (DESs) and their applications. *Chemical reviews* **2014,** *114* (21), 11060-11082.
62. El Achkar, T.; Greige-Gerges, H.; Fourmentin, S., Basics and properties of deep eutectic solvents: a review. *Environmental Chemistry Letters* **2021**, 1-12.
63. Bagh, F. S. G.; Shahbaz, K.; Mjalli, F. S.; Hashim, M. A.; AlNashef, I. M., Zinc (II) chloride-based deep eutectic solvents for application as electrolytes: preparation and characterization. *Journal of Molecular Liquids* **2015,** *204*, 76-83.
64. Zhang, Y.; Han, J.; Liao, C., Insights into the properties of deep eutectic solvent based on reline for Ga-controllable CIGS solar cell in one-step electrodeposition. *Journal of The Electrochemical Society* **2016,** *163* (13), D689.
65. Tome, L. I.; Baiao, V.; da Silva, W.; Brett, C. M., Deep eutectic solvents for the production and application of new materials. *Applied Materials Today* **2018,** *10*, 30-50.
66. Millia, L.; Dall'Asta, V.; Ferrara, C.; Berbenni, V.; Quartarone, E.; Perna, F. M.; Capriati, V.; Mustarelli, P., Bio-inspired choline chloride-based deep eutectic solvents as electrolytes for lithium-ion batteries. *Solid State Ionics* **2018,** *323*, 44-48.
67. Paterno, D.; Rock, E.; Forbes, A.; Iqbal, R.; Mohammad, N.; Suarez, S., Aluminum ions speciation and transport in acidic deep eutectic AlCl3 amide electrolytes. *Journal of Molecular Liquids* **2020,** *319*, 114118.
68. Paterno, D.; Suarez, S., Aluminum Ion Species Transport in Pure and Additive Modulated Deep Eutectic Solvents (DES) Electrolytes. *ECS Transactions* **2020,** *98* (10), 401.
69. Ogawa, H.; Mori, H., Lithium salt/amide-based deep eutectic electrolytes for lithium-ion batteries: electrochemical, thermal and computational study. *Physical Chemistry Chemical Physics* **2020,** *22* (16), 8853-8863.
70. Wu, J.; Liang, Q.; Yu, X.; Lü, Q. F.; Ma, L.; Qin, X.; Chen, G.; Li, B., Deep Eutectic Solvents for Boosting Electrochemical Energy Storage and Conversion: A Review and Perspective. *Advanced Functional Materials* **2021,** *31* (22), 2011102.
71. Di Pietro, M. E.; Mele, A., Deep Eutectics and analogues as electrolytes in batteries. *Journal of Molecular Liquids* **2021**, 116597.
72. Paiva, A.; Craveiro, R.; Aroso, I.; Martins, M.; Reis, R. L.; Duarte, A. R. C., Natural deep eutectic solvents–solvents for the 21st century. *ACS Sustainable Chemistry & Engineering* **2014,** *2* (5), 1063-1071.
73. Wagle, D. V.; Zhao, H.; Baker, G. A., Deep eutectic solvents: sustainable media for nanoscale and functional materials. *Accounts of chemical research* **2014,** *47* (8), 2299-2308.
74. Abbott, A. P.; Harris, R. C.; Ryder, K. S.; D'Agostino, C.; Gladden, L. F.; Mantle, M. D., Glycerol eutectics as sustainable solvent systems. *Green Chemistry* **2011,** *13* (1), 82-90.

75. D'Agostino, C.; Harris, R. C.; Abbott, A. P.; Gladden, L. F.; Mantle, M. D., Molecular motion and ion diffusion in choline chloride based deep eutectic solvents studied by 1 H pulsed field gradient NMR spectroscopy. *Physical Chemistry Chemical Physics* **2011,** *13* (48), 21383-21391.
76. D'Agostino, C.; Gladden, L. F.; Mantle, M. D.; Abbott, A. P.; Essa, I. A.; Al-Murshedi, A. Y.; Harris, R. C., Molecular and ionic diffusion in aqueous–deep eutectic solvent mixtures: probing inter-molecular interactions using PFG NMR. *Physical Chemistry Chemical Physics* **2015,** *17* (23), 15297-15304.
77. Gabriele, F.; Chiarini, M.; Germani, R.; Tiecco, M.; Spreti, N., Effect of water addition on choline chloride/glycol deep eutectic solvents: Characterization of their structural and physicochemical properties. *Journal of Molecular Liquids* **2019,** *291*, 111301.
78. Delso, I.; Lafuente, C.; Munoz-Embid, J.; Artal, M., NMR study of choline chloride-based deep eutectic solvents. *Journal of Molecular Liquids* **2019,** *290*, 111236.
79. Gajardo-Parra, N. F.; Lubben, M. J.; Winnert, J. M.; Leiva, Á.; Brennecke, J. F.; Canales, R. I., Physicochemical properties of choline chloride-based deep eutectic solvents and excess properties of their pseudo-binary mixtures with 1-butanol. *The Journal of Chemical Thermodynamics* **2019,** *133*, 272-284.
80. Tritt-Goc, J.; Rachocki, A.; Bielejewski, M., The solvent dynamics at pore surfaces in molecular gels studied by field-cycling magnetic resonance relaxometry. *Soft Matter* **2014,** *10* (39), 7810-7818.
81. Kruk, D.; Meier, R.; Rossler, E., Translational and rotational diffusion of glycerol by means of field cycling 1H NMR relaxometry. *The Journal of Physical Chemistry B* **2011,** *115* (5), 951-957.
82. Flämig, M.; Hofmann, M.; Fatkullin, N.; Rössler, E., NMR Relaxometry: The Canonical Case Glycerol. *The Journal of Physical Chemistry B* **2020,** *124* (8), 1557-1570.
83. Becher, M.; Wohlfromm, T.; Rössler, E.; Vogel, M., Molecular dynamics simulations vs field-cycling NMR relaxometry: Structural relaxation mechanisms in the glass-former glycerol revisited. *The Journal of Chemical Physics* **2021,** *154* (12), 124503.
84. Bielejewski, M.; Puszkarska, A.; Tritt-Goc, J., Thermal properties, conductivity, and spin-lattice relaxation of gel electrolyte based on low molecular weight gelator and solution of high temperature ionic liquid. *Electrochimica Acta* **2015,** *165*, 122-129.
85. Kruk, D.; Wojciechowski, M.; Verma, Y. L.; Chaurasia, S. K.; Singh, R. K., Dynamical properties of EMIM-SCN confined in a SiO 2 matrix by means of 1 H NMR relaxometry. *Physical Chemistry Chemical Physics* **2017,** *19* (48), 32605-32616.
86. Ordikhani Seyedlar, A.; Stapf, S.; Mattea, C., Nuclear magnetic relaxation and diffusion study of the ionic liquids 1-ethyl-and 1-butyl-3-methylimidazolium bis (trifluoromethylsulfonyl) imide confined in porous glass. *Magnetic Resonance in Chemistry* **2019,** *57* (10), 818-828.
87. Bielejewski, M.; Rachocki, A.; Kaszyńska, J.; Tritt-Goc, J., The gelation influence on diffusion and conductivity enhancement effect in renewable ionic gels based on a LMWG. *Physical Chemistry Chemical Physics* **2018,** *20* (8), 5803-5817.
88. Chen, N.; Zhang, H.; Li, L.; Chen, R.; Guo, S., Ionogel electrolytes for high-performance lithium batteries: A review. *Advanced Energy Materials* **2018,** *8* (12), 1702675.
89. Zavada, T.; Kimmich, R., The anomalous adsorbate dynamics at surfaces in porous media studied by nuclear magnetic resonance methods. The orientational structure factor and Lévy walks. *The Journal of chemical physics* **1998,** *109* (16), 6929-6939.
90. Cheng, X.; Pan, J.; Zhao, Y.; Liao, M.; Peng, H., Gel polymer electrolytes for electrochemical energy storage. *Advanced Energy Materials* **2018,** *8* (7), 1702184.
91. Liang, S.; Yan, W.; Wu, X.; Zhang, Y.; Zhu, Y.; Wang, H.; Wu, Y., Gel polymer electrolytes for lithium ion batteries: Fabrication, characterization and performance. *Solid State Ionics* **2018,** *318*, 2-18.
92. Torrey, H. C., Nuclear spin relaxation by translational diffusion. *Physical Review* **1953,** *92* (4), 962.

93. Brinkkötter, M.; Gouverneur, M.; Sebastião, P.; Chávez, F. V.; Schönhoff, M., Spin relaxation studies of Li+ ion dynamics in polymer gel electrolytes. *Physical Chemistry Chemical Physics* **2017,** *19* (10), 7390-7398.
94. Sinai, Y. G., The limiting behavior of a one-dimensional random walk in a random medium. *Theory of Probability & Its Applications* **1983,** *27* (2), 256-268.
95. Oshanin, G.; Burlatsky, S.; Moreau, M.; Gaveau, B., Behavior of transport characteristics in several one-dimensional disordered systems. *Chemical physics* **1993,** *177* (3), 803-819.
96. Beckmann, P. A., Spectral densities and nuclear spin relaxation in solids. *Physics reports* **1988,** *171* (3), 85-128.
97. Kariyo, S.; Brodin, A.; Gainaru, C.; Herrmann, A.; Hintermeyer, J.; Schick, H.; Novikov, V.; Rössler, E., From simple liquid to polymer melt. Glassy and polymer dynamics studied by fast field cycling NMR relaxometry: Rouse regime. *Macromolecules* **2008,** *41* (14), 5322-5332.